ISSN 2472-1972

IGFBP-3 Induced by Ribotoxic Stress Traffics From the Endoplasmic Reticulum to the Nucleus in Mammary Epithelial Cells

Allyson Agostini-Dreyer,[1] Amanda E. Jetzt,[2] Jennifer Skorupa,[3] Jennifer Hanke,[3] and Wendie S. Cohick[1,2,3]

[1]Graduate Program in Nutritional Sciences, Rutgers, The State University of New Jersey, New Brunswick, New Jersey 08901; [2]Department of Animal Sciences, Rutgers, The State University of New Jersey, New Brunswick, New Jersey 08901; and [3]Graduate Program in Endocrinology and Animal Biosciences, Rutgers, The State University of New Jersey, New Brunswick, New Jersey 08901

ORCiD numbers: 0000-0001-9312-0121 (A. E. Jetzt); 0000-0002-6747-1558 (W. S. Cohick).

IGF-binding protein (IGFBP)-3 is a multifunctional protein that can exert IGF-independent effects on apoptosis. Anisomycin (ANS) is a potent inducer of IGFBP-3 production in bovine mammary epithelial cells (MECs), and knockdown of IGFBP-3 attenuates ANS-induced apoptosis. IGFBP-3 is present in the nucleus and the conditioned media in response to ANS. The goal of this study was to determine whether ribotoxic stress induced by ANS or a second ribotoxin, deoxynivalenol (DON), specifically regulates transport of IGFBP-3 to the nucleus and to determine the pathway by which it traffics. In ribotoxin-treated cells, both endogenous IGFBP-3 and transfected IGFBP-3 translocated to the nucleus. Inhibition of the nuclear transport protein importin-β with importazole reduced ribotoxin-induced nuclear IGFBP-3. Immunoprecipitation studies showed that ANS induced the association of IGFBP-3 and importin-β, indicating that ribotoxins specifically induce nuclear translocation via an importin-β–dependent mechanism. To determine whether secretion of IGFBP-3 is required for nuclear localization, cells were treated with Pitstop 2 or brefeldin A to inhibit clathrin-mediated endocytosis or overall protein secretion, respectively. Neither inhibitor affected nuclear localization of IGFBP-3. Although the IGFBP-3 present in both the nucleus and conditioned media was glycosylated, secreted IGFBP-3 exhibited a higher molecular weight. Deglycosylation experiments with endoglycosidase Hf and PNGase indicated that secreted IGFBP-3 completed transit through the Golgi apparatus, whereas intracellular IGFBP-3 exited from the endoplasmic reticulum before transit through the Golgi. In summary, ANS and DON specifically induced nuclear localization of non-secreted IGFBP-3 via an importin-β–mediated event, which may play a role in their ability to induce apoptosis in MECs.

Copyright © 2019 Endocrine Society

This article has been published under the terms of the Creative Commons Attribution Non-Commercial, No-Derivatives License (CC BY-NC-ND; https://creativecommons.org/licenses/by-nc-nd/4.0/).

Freeform/Key Words: IGFBP-3, glycosylation, nuclear localization, deoxynivalenol, anisomycin

In the dairy cow, milk output over a lactation cycle is a function of mammary epithelial cell (MEC) number over time [1]. Daily milk yield is highest approximately 3 to 6 weeks after calving, when secretory cell number and secretory activity per cell have peaked. The ensuing decline in milk yield is due to loss of MECs by apoptosis [2, 3]. At the cellular level, altering

Abbreviations: ANS, anisomycin; CM, conditioned media; CME, clathrin-mediated endocytosis; DON, deoxynivalenol; Endo H, endoglycosidase Hf; ER, endoplasmic reticulum; ERAD, endoplasmic reticulum-associated degradation; GFP, green fluorescent protein; IGFBP, IGF-binding protein; IGFBP-3-GFP, GFP-tagged IGF-binding protein-3; MEC, mammary epithelial cell; NLS, nuclear localization signal; SDS-PAGE, sodium dodecyl sulfate polyacrylamide gel electrophoresis; SF, serum-free; siRNA, small interfering ribonucleic acid; Tf-FITC, fluorescently labeled transferrin.

Received 8 October 2018
Accepted 11 December 2018
First Published Online 24 December 2018

March 2019 | Vol. 3, Iss. 3
doi: 10.1210/js.2018-00330 | Journal of the Endocrine Society | 517–536

the balance between anti-apoptotic and proapoptotic signals in favor of survival has the potential to improve lactational persistency and thus increase total lactation yield [4].

The IGF system is a major regulator of proliferation and survival in the mammary gland. It is composed of two ligands, two receptors, and six IGF-binding proteins (IGFBPs) that modulate IGF activity. IGFBP-3 is the major transporter of IGF in the circulation [5]. At the cellular level, it has multiple functions depending on cell type and cellular context. Numerous studies have reported that IGFBP-3 exerts apoptotic effects through both IGF-dependent and IGF-independent mechanisms. Although IGFBP-3 is a secreted protein, it contains a nuclear localization signal (NLS) and is detected in the nucleus of multiple cell lines, suggesting an intracrine function [6–11].

The intrinsic apoptotic pathway is activated by ribotoxins such as anisomycin (ANS) and deoxynivalenol (DON). These proteins target the ribosome to elicit a conserved cellular response referred to as *ribotoxic stress,* which is characterized by activation of mitogen-associated protein kinase pathways and subsequent apoptosis [12, 13]. Previous work from our laboratory showed that IGFBP-3 plays a role in the ability of ANS to induce intrinsic apoptosis in bovine MECs independent of IGF-I [6]. Further, IGFBP-3 is detected in the nucleus of ANS-treated cells, leading us to hypothesize that cellular localization contributes to the regulation of the biological function of IGFBP-3. However, the mechanism by which it localizes to the nucleus in these cells remains unclear. Studies in osteosarcoma and prostate cancer cells have indicated that IGFBP-3 is internalized through several different mechanisms [9, 14], leading to the proposal that nuclear IGFBP-3 arises from the secreted protein. However, when prostate cancer cells are transfected with IGFBP-3 lacking the signal peptide required for secretion, IGFBP-3 is still found in the nucleus and can induce apoptosis, suggesting that secretion is not a required event for nuclear localization [15, 16]. The objective of the current study was to elucidate the mechanism for nuclear import of IGFBP-3 during apoptosis in bovine MECs.

1. Materials and Methods

A. Reagents

DMEM-H with high glucose (4.5 g/L D-glucose), penicillin, streptomycin, 10% neutral buffered formalin, and Hoechst 33342 were purchased from Thermo Fisher Scientific (Waltham, MA). Phenol red-free DMEM low-glucose media, insulin, BSA, sodium selenite, imidazole, ANS, DON, and brefeldin A were purchased from Sigma-Aldrich (St. Louis, MO). Gentamycin was obtained from Amresco (Solon, OH). Fetal bovine serum was obtained from Atlanta Biologicals (Flowery Branch, GA). The enzymes endoglycosidase H_f (Endo H) and PNGase F were purchased from New England Biolabs (Ipswich, MA). Importazole was obtained from Millipore (Billerica, MA). Superfect transfection reagent was purchased from Qiagen (Germantown, MD). Custom SmartPool small interfering ribonucleic acid (siRNA) for bovine IGFBP-3 and nontargeting control siRNA (scramble) were obtained from Dharmacon (Lafayette, CO). *Trans*IT-TKO transfection reagent was purchased from Mirus Bio (Madison, WI). Fluorescently labeled transferrin (Tf-FITC) was purchased from Rockland Inc (Gilbertsville, PA). Pitstop 2 was obtained from Cellagen Technology (San Diego, CA). Antibodies used in this work are described in Table 1. Cleaved caspase-3 (Asp 175), RRID:AB_2341188 [17]; cleaved caspase-7 (Asp 198), RRID: AB_2068144 [18]; and PARP, RRID:AB_2160739 [19], were obtained from Cell Signaling Technology (Danvers, MA). HSP60, RRID:AB_733032 [20], and anti-NTF97/importin-β [3E9], RRID:AB_2133989 [21], were purchased from Abcam (Cambridge, MA). Lamin A/C (H-110), RRID:AB_648154 [22], was from Santa Cruz (Dallas, TX). THE His Tag, RRID: AB_914704 [23], was obtained from Genscript (Piscataway, NJ). HRP horse anti-mouse IgG, RRID:AB_2336177 [24], was purchased from Vector Laboratories (Burlingame, CA) and anti-rabbit IgG HRP-linked, RRID:AB_772206 [25], was from GE Healthcare (Chicago, IL).

Table 1. Antibody Table

Peptide/ Protein Target	Antigen Sequence (if known)	Name of Antibody	Manufacturer, Catalog No., and/or Name of Individual Providing the Antibody	Species Raised in; Monoclonal or Polyclonal	Dilution Used	RRID
Bovine IGFBP-3	Full-length bovine IGFBP-3	Rabbit anti-bovine IGFBP-3	Produced in-house	Rabbit; poly	1:5000 (WB) 1:250 (IP)	AB_2752245 [27]
Cleaved caspase-3	Synthetic peptide corresponding to amino-terminal residues adjacent to Asp175 in human caspase-3	Cleaved caspase-3 (Asp175)	Cell Signaling Tech 9661	Rabbit; poly	1:1000 (WB)	AB_2341188 [17]
Cleaved caspase-7	Synthetic peptide corresponding to amino-terminal residues surrounding Asp198 in human caspase-7	Cleaved caspase-7 (Asp198)	Cell Signaling Tech 9491	Rabbit; poly	1:1000 (WB)	AB_2068144 [18]
PARP	Synthetic peptide corresponding to the caspase cleavage site in PARP	PARP	Cell Signaling Tech 9542	Rabbit; poly	1:1000 (WB)	AB_2160739 [19]
HSP60	Synthetic peptide corresponding to amino acids 31–50 of human Hsp60	Anti-HSP60	Abcam ab31115	Rabbit; poly	1:20,000 (WB)	AB_733032 [20]
Lamin A/C	aa213–340 of human lamin A	Lamin A/C (H-110)	Santa Cruz sc-20681	Rabbit; poly	1:10,000 (WB)	AB_648154 [22]
His-tag	Synthetic peptide HHHHHH coupled to KLH	THE His Tag	Genscript A00186	Mouse; mono	1:250 (IP)	AB_914704 [23]
Importin-β	Full-length native bovine protein	Anti-NTF97/importin-β [3E9]	Abcam ab2811	Mouse; mono	1:1000 (WB) 1:500 (IP)	AB_2133989 [21]
	Mouse IgG	HRP horse anti-mouse IgG	Vector PI-2000	Horse	Varied	AB_2336177 [24]
	Rabbit IgG	Anti-rabbit IgG, HRP linked	GE Healthcare NA934V	Donkey	Varied	AB_772206 [25]

Abbreviations: IP, immunoprecipitation; WB, western blot.

B. Cell Culture

The bovine MEC line MAC-T [26] was routinely maintained and plated for experiments as previously described [10].

C. Generation of Bovine IGFBP-3 Antisera

To generate IGFBP-3 antigen for antisera production, MAC-T cells were transfected with a plasmidencoding bovine IGFBP-3-His cDNA as previously described [10]. Cells were transfected using SuperFect (Qiagen) combined with plasmid in a 1:5 ratio in 100-mm^2 dishes. Following a 24-hour recovery in serum-containing media, cells were rinsed twice in PBS and incubated with fresh serum-free (SF) DMEM-H (5 mL per plate) for 72 hours. Media were collected and filtered through a 0.22-μm polyethersulfone bottle top filter (Corning, Tewksbury, MA) to remove dead cells and debris and were then stored at 4°C until use. Chromatography columns (Bio-Rad, Hercules, CA) were each loaded with 1 mL of Ni-NTA agarose (Qiagen), supernatant was allowed to flow through, and beads were resuspended in 4 mL of bind buffer (300 mM NaCl, 50 mM Na_3HPO_4, 10 mM imidazole; pH, 8). The supernatant was again allowed to flow through and discarded. Ten milliliters of conditioned media (CM) was added per column and incubated for 2 hours at 4°C on a rotating platform; beads were then allowed to settle by gravity, and media were allowed to flow through. Columns were washed three times with wash buffer (300 mM NaCl, 50 mM Na_3HPO_4, 20 mM imidazole; pH, 8). Bound protein was eluted with 3 × 1 mL volumes of elution buffer (300 mM NaCl, 50 mM Na_3HPO_4, 250 mM imidazole; pH, 8). Primary elutions containing IGFBP-3 were concentrated in Amicon Ultra YM10 centrifugal concentrators (Millipore). Buffer exchange was used to dilute the elution buffer to achieve an imidazole concentration below 50 mM. Primary elutions (30 μL) were run under reducing and denaturing conditions on a 12.5% polyacrylamide gel. The gel was then fixed and stained using a silver stain kit according to manufacturer's instructions (Bio-Rad) to determine protein purity. Concentrated IGFBP-3 was sterilized by passage through a syringe filter (Macherey-Nagel, Bethlehem, PA). Samples were then stored overnight at −20°C or used as an antigen on the same day.

The antibody was generated in naive New Zealand white rabbits. Animal care was performed in accordance with guidelines from the Rutgers Institutional Animal Care and Use Committee and complied with National Institutes of Health Policy. To generate the antibody, animals received an initial subcutaneous injection of 500 μg IGFBP-3 followed by two booster injections on weeks 5 (200 μg) and 14 (100 μg). Nonimmune serum was collected before the first dose and showed lack of cross-reactivity with bovine IGFBP-3. The initial dose of IGFBP-3 was mixed with an equal volume of Freund's complete adjuvant. Subsequent doses were mixed with Freund's incomplete adjuvant. All doses were administered at four subcutaneous injection sites. Blood was collected, and serum was isolated seven times over the course of 22 weeks. To test the bleeds for IGFBP-3 specificity, biological samples containing IGFBP-3 were immunoblotted with the antiserum, and the bleed that produced the strongest and most specific signal was selected [27]. As shown in Fig. 1, the antibody recognized several molecular weight forms of IGFBP-3 in whole-cell lysates (WCLs) and CM collected from MAC-T cells treated with ANS. Specificity for IGFBP-3 was demonstrated by showing that these bands were significantly reduced by treatment with IGFBP-3 siRNA. In addition, no additional forms of IGFBP secreted by MAC-T cells [28] or other nonspecific bands were detected by the antiserum.

D. Caspase-3/7 Assay

MAC-T cells were treated ± toxin and then assayed for caspase-3 and caspase-7 cleavage with the SensoLyte Homogeneous AMC Caspase-3/7 Assay Kit (AnaSpec, Fremont, CA) according to the manufacturer's specifications.

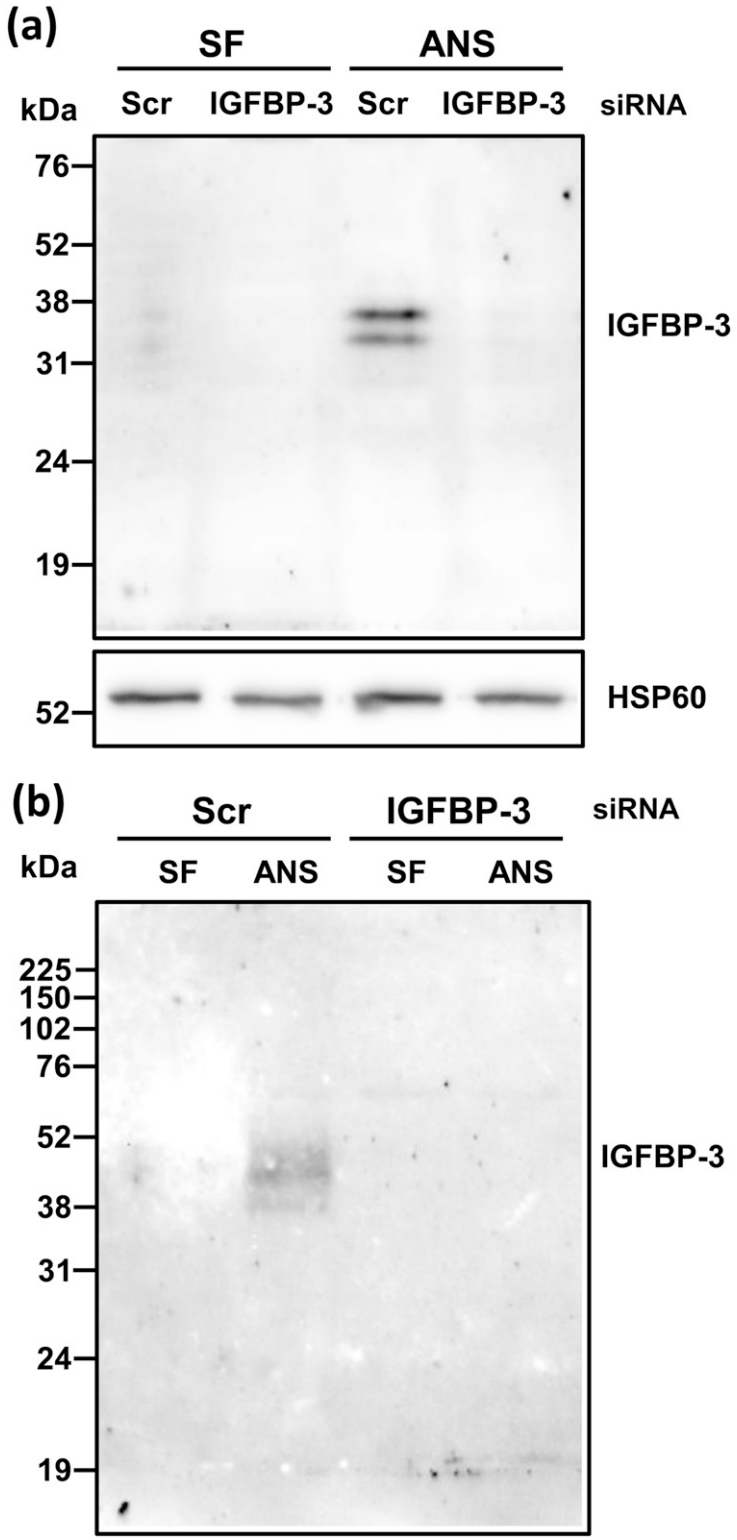

Figure 1. Bovine IGFBP-3 polyclonal antibody specifically detects IGFBP-3 in whole cell lysates (WCLs) and CM of MAC-T cells. MAC-T cells were transfected with 50 nM of IGFBP-3 or Scr siRNA for 48 h, serum starved overnight, and treated with ± 0.1 μM of ANS for 6 h (WCLs) or 18 h (CM). (a) WCLs (40 μg) and (b) CM (100 μL) were immunoblotted for IGFBP-3 [27]. HSP60 served as a loading control for WCLs. Scr, scramble.

E. RNA Isolation and Reverse Transcription-Quantitative Polymerase Chain Reaction

RNA was isolated using the NucleoSpin RNA Plus isolation kit (Macherey-Nagel). RNA integrity was assessed by visualization of 28 and 18S ribosomal bands after agarose gel electrophoresis. RNA (1 μg) was reverse transcribed with the High-Capacity Reverse Transcription Kit (Thermo Fisher Scientific). Quantitative polymerase chain reaction primer sets were developed using PrimerQuest (IDT, Coralville, IA) and were purchased from Sigma-Aldrich. For IGFBP-3, primers were forward, 5′-CAGAGCACAGACACCCAGAA-3′, and reverse, 5′-GGAACTTGAGGTGGTTCAGC-3′. For cyclophilin, primers were forward, 5′-GAGCACTGGAGAGAAAGGATTTGG-3′, and reverse, 5′-TGAAGTCACCACCCTGGCA-CATAA-3′. Primers were validated as previously described [10]. The amplification efficiencies for the primers were 99.8% ± 0.3% for IGFBP-3 and 100% ± 0.01% for cyclophilin (mean ± SD for three independent curves). Samples were diluted 1:4, and 5 μL was amplified in a 20-μL reaction containing 10 μL Power SYBR Green (Thermo Fisher Scientific), 4 μL H_2O, and 0.5 μL (0.25 μM IGFBP-3, 0.125 μM cyclophilin) of each gene-specific primer. Reactions were run on the Applied Biosystems StepOnePlus system (Applied Biosystems, Foster City, CA) using cycle parameters of 95°C for 10 minutes, followed by 40 cycles of 95°C for 15 seconds and 60°C for 1 minute. Data were analyzed using the relative $\Delta\Delta$CT method with cyclophilin as the housekeeping gene. PCR products were verified by melt curve analysis.

F. Cell Lysis and Immunoblotting

Cytosolic and nuclear fractions were obtained as described [10], and WCLs were obtained as described [29]. Lysates were assayed for protein concentration with the Bio-Rad Protein Assay and immunoblotted as previously described [30] with the following exceptions: blocking buffer contained 0.1% Tween 20 (v/v) and 5% nonfat dried milk (w/v), secondary antibody incubation was 1 hour, and peroxidase activity was detected with ECL Prime (GE Healthcare). Chemiluminescence was detected with the FluorChem FC2 imaging system (ProteinSimple, San Jose, CA).

G. Immunoprecipitation

Cell lysates (500 μg) were collected in Active Motif Complete Lysis Buffer (Carlsbad, CA) and incubated with antibody on a rotating platform overnight at 4°C. Samples were added to 20 μL of prewashed protein G beads (Millipore) and incubated on a rotating platform for 2 hours at 4°C. Beads were then washed three times with PBS, and bound proteins were eluted in 2× Laemmli buffer under reducing conditions at 95°C for 5 minutes. The supernatant was separated by sodium dodecyl sulfate polyacrylamide gel electrophoresis (SDS-PAGE) and immunoblotted.

H. siRNA Transfection

MAC-T cells were plated and transfected with 50 nM of IGFBP-3 siRNA oligos or non-targeting control (scramble) siRNA as previously described [10]. After 48 hours, cells were washed and incubated overnight in SF media and then treated ± ribotoxin to induce apoptosis.

I. Construction of Green Fluorescent Protein-Tagged IGFBP-3

A plasmid containing the signal sequence followed by the full-length protein coding sequence of bovine IGFBP-3 was used to generate green fluorescent protein (GFP)-tagged protein [29]. The GFP-tag was added as described for the construction of IGFBP-3-His [10] with the following changes. *Xho*I and *BamHI* restriction sites were added to the 5′ and 3′ ends of bovine IGFBP-3, respectively, producing a 900-bp fragment. The reverse primer was 5′-ACAAGTGGATCCACCTTGCTCTCCATGCTGTAGCAGTC-3′. The cycling parameters were

94°C for 2 minutes; 30 cycles of 94°C for 1 minute, 50°C for 1 minute, 68°C for 1 minute; and 68°C for 10 minutes. BP3 (insert) and pEGFP-N1 (vector) were digested with *Xho*I and *Bam*HI.

J. Fluorescence Microscopy

MAC-T cells were plated in complete media on eight-well μ-slides (Ibidi, Martinsried, Germany). For transfection, cells were plated at 3.5×10^4 cells/cm^2. The next day, subconfluent cells were transfected with a plasmid encoding cDNA for GFP-tagged IGFBP-3 (IGFBP-3-GFP), IGFBP-3-His, or pEGFP-N1 using SuperFect (Qiagen) in a 1:10 ratio as previously described [10]. After a 24-hour recovery in serum-containing media, cells were rinsed twice in PBS and incubated with fresh SF DMEM-H for 1 hour, then treated as indicated in the figure legends. Cells were fixed with 10% neutral buffered formalin (Thermo Fisher Scientific). Nuclei were stained with Hoechst 33342 (Thermo Fisher Scientific). Cells were stored in mounting media (Ibidi), and images were acquired with an Olympus FSX100 microscope (Olympus, Shinjuku, Tokyo, Japan) at 40× and 60× magnifications.

K. Endo H and PNGase Digestion

WCL (50 μg), cytosolic fraction (50 μg), nuclear fraction (30 μg), or CM (100 μL concentrated to 20 μL) were digested with Endo H (New England Biolabs) in a reaction that included 2500 U of enzyme and GlycoBuffer 3. Reactions were incubated at 37°C for 20 hours and then analyzed by SDS-PAGE. WCL (50 μg) or CM (100 μL concentrated to 20 μL) were digested with PNGase F (New England Biolabs) in a reaction that included 1000 U of enzyme, 1% NP-40, and GlycoBuffer 2. Reactions were incubated at 37°C for 20 hours and then analyzed with SDS-PAGE.

L. Statistical Analyses

Statistical analyses were performed using GraphPad Prism 7.0 (La Jolla, CA).

2. Results

A. ANS and DON Induced IGFBP-3 Expression, Which Played a Role in Their Ability to Induce Apoptosis

We previously reported that ANS induced apoptosis as well as IGFBP-3 expression in MAC-T cells and that ANS was less effective at inducing apoptosis when IGFBP-3 was reduced with siRNA [6]. To test whether this is part of a universal ribotoxic stress response, we compared the response of cells to ANS with the response to DON, a trichothecene mycotoxin that also inhibits the peptidyltransferase reaction and induces the ribotoxic stress signaling pathway [31]. Similar to treatment with ANS, treatment with DON also induced apoptosis [Fig. 2(a)] and IGFBP-3 expression at both the mRNA level [Fig. 2(b)] and the protein level [Fig. 2(c)]. Knockdown of IGFBP-3 with siRNA before treatment with either ANS or DON significantly attenuated their ability to induce apoptosis as measured by western immunoblotting using antibodies that recognize the cleaved forms of PARP and caspases 3 and 7 [Fig. 2(d) and 2(e)]. Therefore, IGFBP-3 appears to be part of a universal stress response to ribotoxins in MAC-T cells.

B. ANS and DON Induced Nuclear Localization of IGFBP-3 Mediated by Importin-β

In our previous work, we showed that endogenous IGFBP-3 localized to the nucleus in cells treated with ANS. In the present work, IGFBP-3 was low to undetectable in both nuclear and cytosolic fractions from untreated cells, whereas following treatment with either ANS or DON, IGFBP-3 was present in both the nucleus and the cytoplasm [Fig. 3(a)]. The presence of

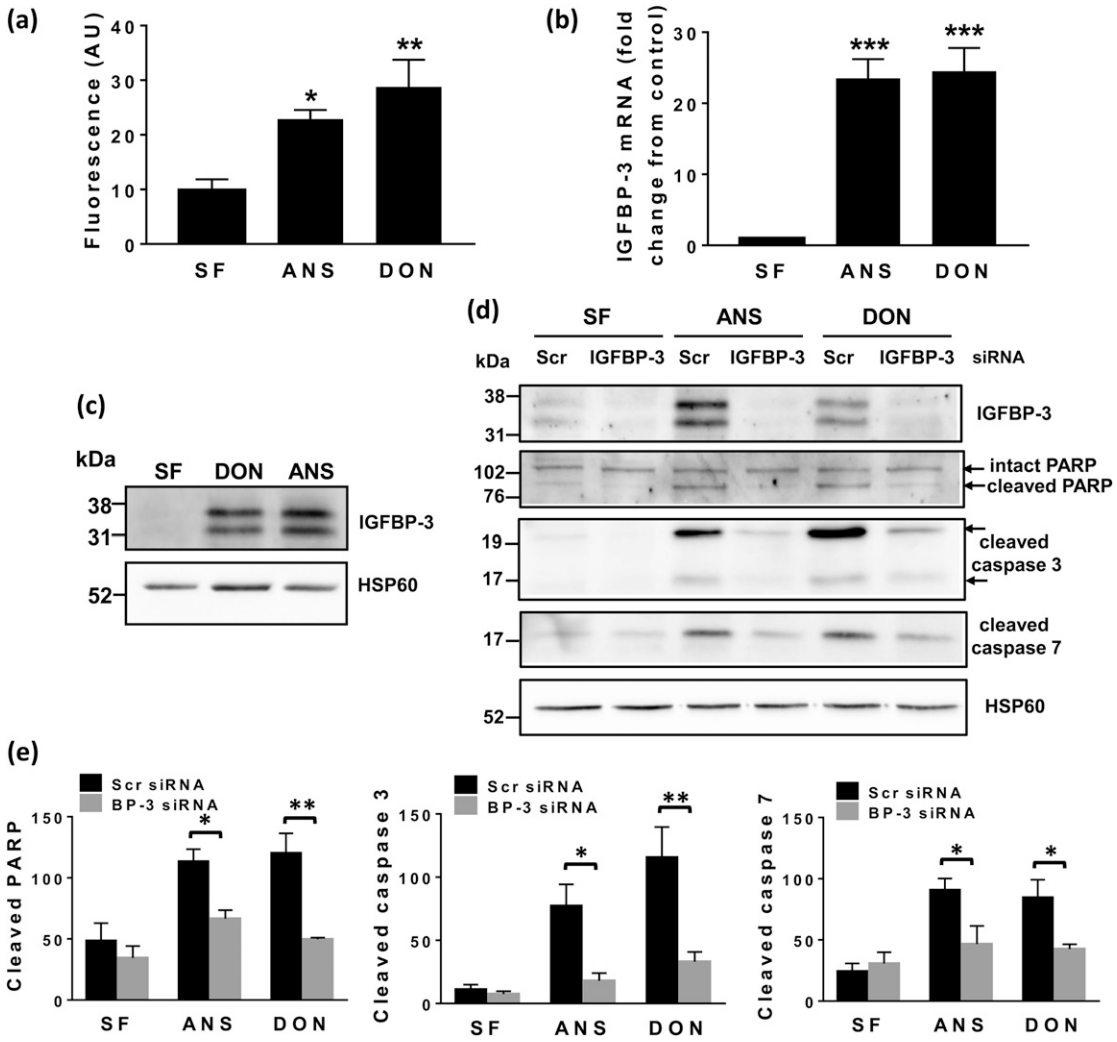

Figure 2. Induction of IGFBP-3 expression was required for ribotoxins to induce apoptosis. (a–c) Confluent MAC-T cells were serum starved overnight and treated with 0.1 μM ANS, 1.0 μg/mL DON, or SF media as indicated. (a) Caspase-3/7 activation was measured with the SensoLyte Caspase-3/7 Assay (AnaSpec) after 6 hours of treatment; (b) total RNA was collected and analyzed for IGFBP-3 mRNA by Reverse transcription-quantitative polymerase chain reaction with data corrected for cyclophilin levels after 4 h of treatment. (a and b) Bars represent mean ± SEM of four individual experiments, with treatment measured in triplicate within each experiment. Data were analyzed using one-way ANOVA with the Tukey multiple comparisons *post hoc* test. *$P < 0.05$; **$P < 0.01$; ***$P < 0.001$ compared with SF control. (c) Whole-cell lysates were collected after 6 h of treatment, and 40 μg was separated using sodium dodecyl sulfate polyacrylamide gel electrophoresis and immunoblotted for IGFBP-3. HSP60 was used as a loading control. Data are representative of four independent experiments. (d) MAC-T cells were transfected with 50 nM of IGFBP-3 or Scr siRNA for 48 h, serum starved overnight, and treated with 0.1 μM ANS, 1.0 μg/mL DON, or SF media for 6 h. Whole-cell lysates (40 μg) were separated using sodium dodecyl sulfate polyacrylamide gel electrophoresis and immunoblotted for IGFBP-3 and cleaved PARP, caspase-3, and caspase-7. HSP60 was used as a loading control. (e) Western blots from three experiments were quantitated by densitometry. Bars represent mean ± SEM. Data were analyzed by two-way ANOVA with the Sidak multiple comparisons *post hoc* test. *$P < 0.05$; **$P < 0.01$. AU, arbitrary units; Scr, scramble.

IGFBP-3 in the nucleus could be a function of passive diffusion through the nuclear pores, which can occur for proteins with a molecular weight <45 kDa. To test this, cells were transfected with GFP-tagged IGFBP-3, which has a molecular weight of approximately 64 kDa. Under SF conditions, IGFBP-3-GFP was detected primarily in the cytosol; however,

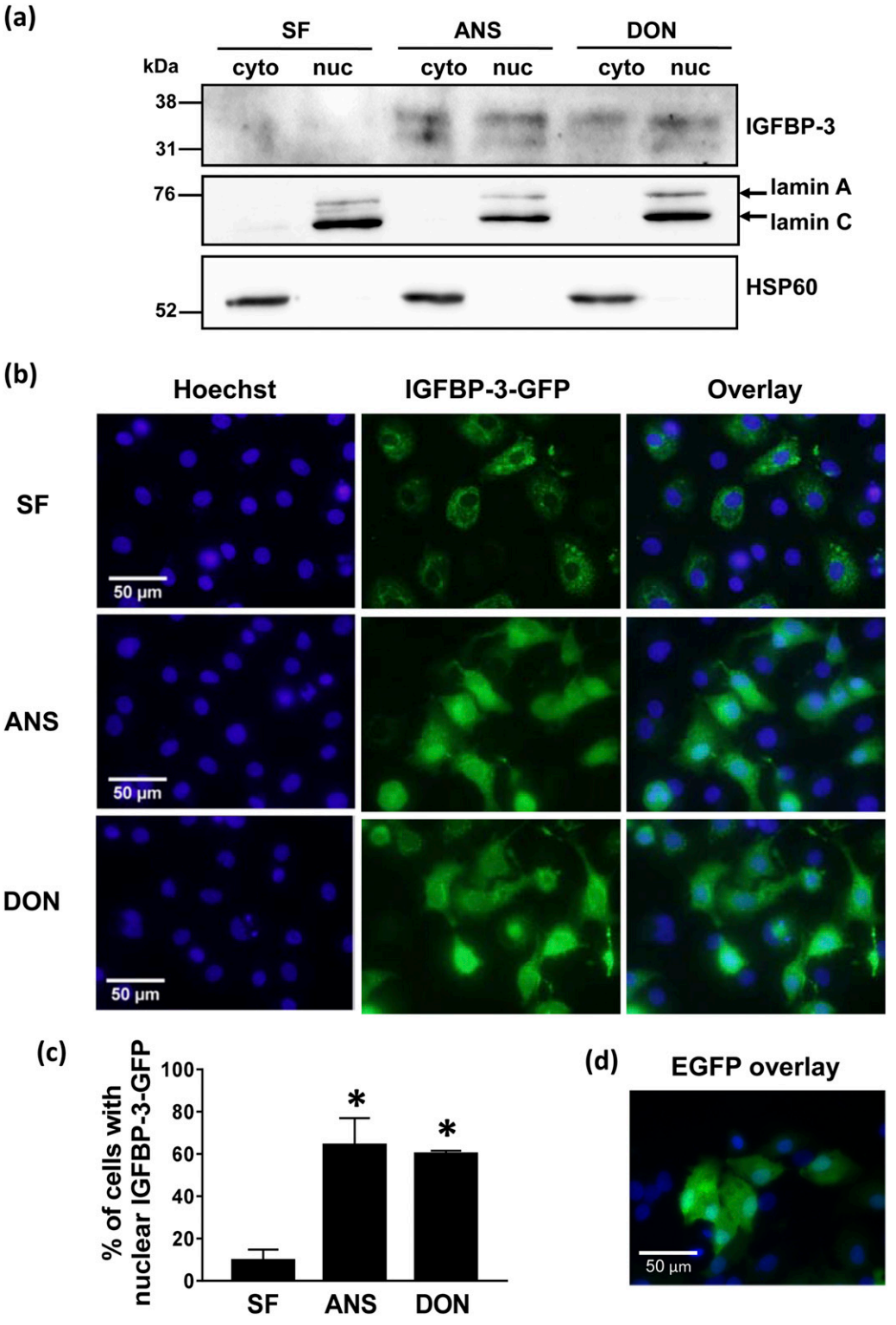

Figure 3. ANS and DON induced nuclear localization of IGFBP-3. (a) MAC-T cells were treated for 6 h ± 0.1 µM ANS or 1 µg/mL DON, then fractionated and immunoblotted for IGFBP-3. Lamin A/C and HSP60 served as controls for cytoplasmic (cyto) and nuclear (nuc) loading, respectively. Results are representative of three independent experiments. (b) MAC-T cells transfected with IGFBP-3-GFP were treated for 2 h ± 0.1 µM ANS or 1 µg/mL DON. Cells were fixed in formalin, and then nuclei were stained with Hoechst. Images were acquired with an Olympus FSX100 microscope at 40× magnification. Images are

representative of two independent experiments. (c) For the two experiments, approximately 200 transfected cells were counted to determine the percentage that contained nuclear IGFBP3-GFP. Bars represent mean ± SD. Data were analyzed using one-way ANOVA with the Tukey multiple comparisons *post hoc* test. *$P < 0.05$ compared with SF control. (d) As a control, cells were transfected with EGFP-plasmid alone and nuclei were stained with Hoechst. EGFP, pEGFP-N1 plasmid.

nuclear localization was observed within 2 hours of exposure to ANS or DON, indicating that active transport is required and is specifically induced by ribotoxin [Fig. 3(b)]. Quantification indicated that in cells treated with either ANS or DON, approximately 60% of transfected cells exhibited nuclear localization compared with 10% of untreated cells [Fig. 3(c)]. Transfection with a control plasmid encoding EGFP protein alone showed GFP equally distributed between the cytoplasm and the nucleus [Fig. 3(d)].

To determine whether nuclear transport of IGFBP-3 is mediated by importin-β in MAC-T cells as has been reported in other cell lines [14, 32], cells were treated ± ribotoxin with or without importazole, a small-molecule inhibitor of importin-β. As shown in Fig. 4(a) and 4(b), ribotoxin-induced nuclear localization of IGFBP-3-GFP was significantly attenuated by importazole, indicating that IGFBP-3 utilizes importin-β for nuclear import. Quantification indicated that <10% of transfected cells exhibited nuclear IGFBP-3-GFP under SF, importazole, or importazole + toxin treatment, compared with 60% to 80% of cells with ANS or DON [Fig. 4(c)]. To determine whether ANS induces a physical association between endogenous IGFBP-3 and importin-β, cells were treated ± ANS, immunoprecipitated with IGFBP-3 or importin-β antibody, and immunoblotted with the opposite antibody. As shown in Fig. 5(a) and 5(b), IGFBP-3 and importin-β coimmunoprecipitated only in ANS-treated cells. Because untreated cells contain very low levels of endogenous IGFBP-3, cells were transfected with IGFBP-3-His to determine whether the association required ANS treatment [Fig. 5(c)]. Immunoprecipitation experiments indicated that exogenous IGFBP-3 and importin-β associated only in cells that were treated with ANS, even though untreated controls contained similar amounts of IGFBP-3.

C. IGFBP-3 Was Not Secreted Before Nuclear Localization

To determine whether secreted IGFBP-3 is reinternalized then directed to the nucleus as reported by others, Pitstop 2, an inhibitor of clathrin-mediated endocytosis (CME), was used [33]. To confirm that Pitstop 2 successfully prevents endocytosis, cells were treated with Tf-FITC, which is known to use CME for cellular entry. In the absence of inhibitor, Tf-FITC was distributed throughout the cell; however, treatment with Pitstop 2 resulted in an absence of intracellular Tf-FITC, demonstrating inhibition of endocytosis [Fig. 6(a)]. Cells were then treated with ANS with or without the inhibitor. Treatment with Pitstop 2 did not reduce nuclear accumulation of IGFBP-3 or increase its accumulation in CM, both of which would be expected to occur if nuclear IGFBP-3 arose from secreted protein [Fig. 6(b)]. It was also observed that IGFBP-3 in CM ran at a higher molecular weight than did nuclear IGFBP-3.

Because secreted protein can be internalized via multiple mechanisms, a second approach was used. Cells were treated with ANS or DON ± brefeldin A, which inhibits endoplasmic reticulum (ER) to Golgi transport, effectively blocking secretion. Cells were then fractionated and immunoblotted for IGFBP-3. Treatment with brefeldin A did not affect nuclear accumulation of endogenous IGFBP-3, indicating that it does not need to be secreted before localizing to the nucleus. Analysis of IGFBP-3 in the CM of cells treated with brefeldin A confirmed that secretion of IGFBP-3 was successfully inhibited [Fig. 7(a) and 7(b)]. Similar to the western immunoblotting results described for Fig. 6(b), IGFBP-3 in CM ran at a higher molecular weight than nuclear IGFBP-3 did. Movement of IGFBP-3 was also visualized by fluorescence microscopy [Fig. 7(c) and 7(d)]. Cells were transfected with IGFBP-3-GFP and treated with ANS or DON ± brefeldin A. Treatment with brefeldin A did not prevent movement of IGFBP-3-GFP to the nucleus in response to either ribotoxin.

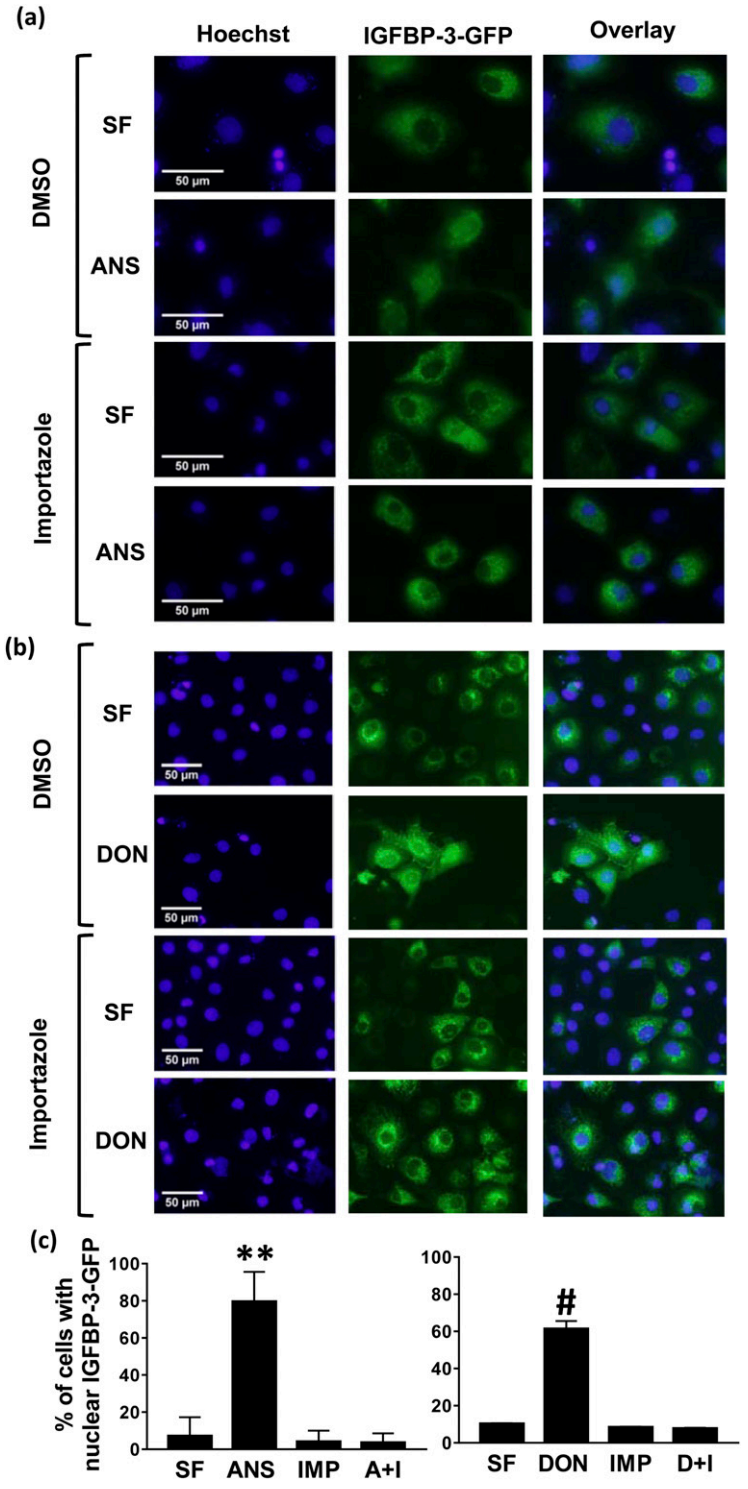

Figure 4. Importazole reduced nuclear import of IGFBP-3-GFP. Cells transfected with IGFBP-3-GFP were treated for 4 h ± (a) 0.1 μM ANS or (b) 1 μg/mL DON ± 40 μM importazole. Cells were fixed in formalin, and then nuclei were stained with Hoechst. Images were acquired with an Olympus FSX100 microscope at (a) 60× and (b) 40× magnifications. Images are representative of two independent experiments. (c) For the two experiments, approximately 200 transfected cells were counted to determine the percentage that contained nuclear IGFBP3-GFP. Bars represent mean ± SD. Data were analyzed using one-way ANOVA with the Tukey multiple comparisons *post hoc* test. $^{**}P < 0.01$; $\#P < 0.0001$ compared with SF control. A+I, ANS + IMP; D+I, DON + IMP; DMSO, dimethyl sulfoxide; IMP, importazole.

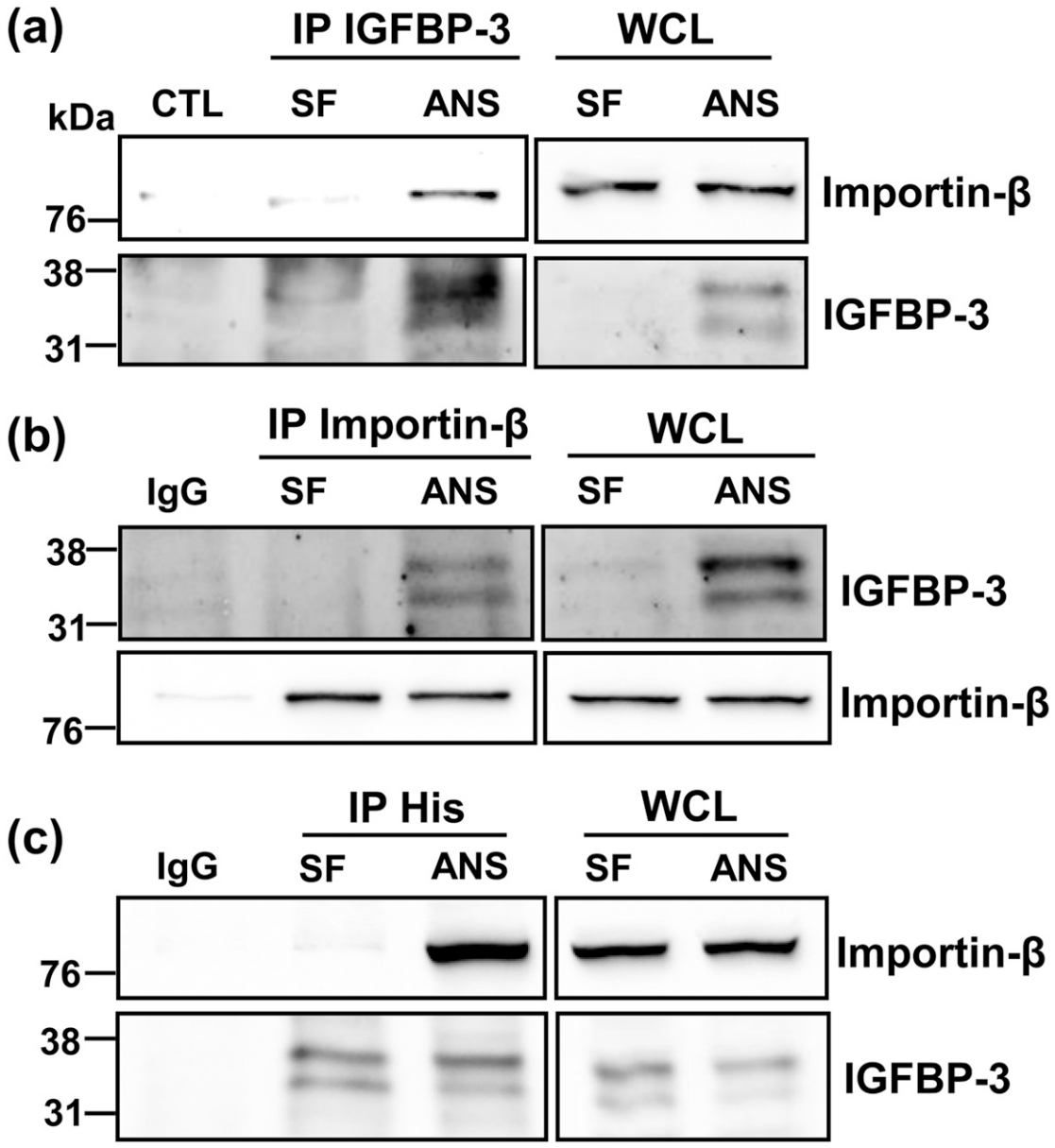

Figure 5. IGFBP-3 was associated with importin-β in response to ANS treatment. MAC-T cells were treated for 8 h ± 0.1 μM ANS. WCLs were collected, and IGFBP-3 and importin-β were immunoprecipitated (IP) with (a) anti–IGFBP-3 antibody or (b) importin-β antibody, respectively. (c) MAC-T cells transfected with IGFBP-3-His were treated for 1 h ± 0.1 μM ANS. IGFBP-3 was IP with an anti–His-tag antibody. (a) Rabbit nonimmune serum (CTL) and (b, c) mouse IgG served as controls. Results represent three independent experiments.

D. Secreted and Intracellular IGFBP-3 Were Differentially Glycosylated

The data obtained with Pitstop 2 and brefeldin A suggest that in the MAC-T cell system, IGFBP-3 does not need to be secreted and reinternalized to reach the nucleus. The molecular weight of nuclear IGFBP-3 suggests that the protein was glycosylated. To confirm this, cells were transfected with IGFBP-3-His, treated with ANS, and fractionated into nuclear and cytoplasmic compartments. Fractions were treated with Endo H and analyzed by SDS-PAGE. As shown in Fig. 8(a), IGFBP-3-His ran as a doublet between 37 and 39 kDa in both cytosolic and nuclear fractions. Digestion of either fraction with Endo H resulted in a single faster-migrating band approximately the size of nonglycosylated IGFBP-3, indicating that both cytoplasmic and nuclear IGFBP-3 were glycosylated.

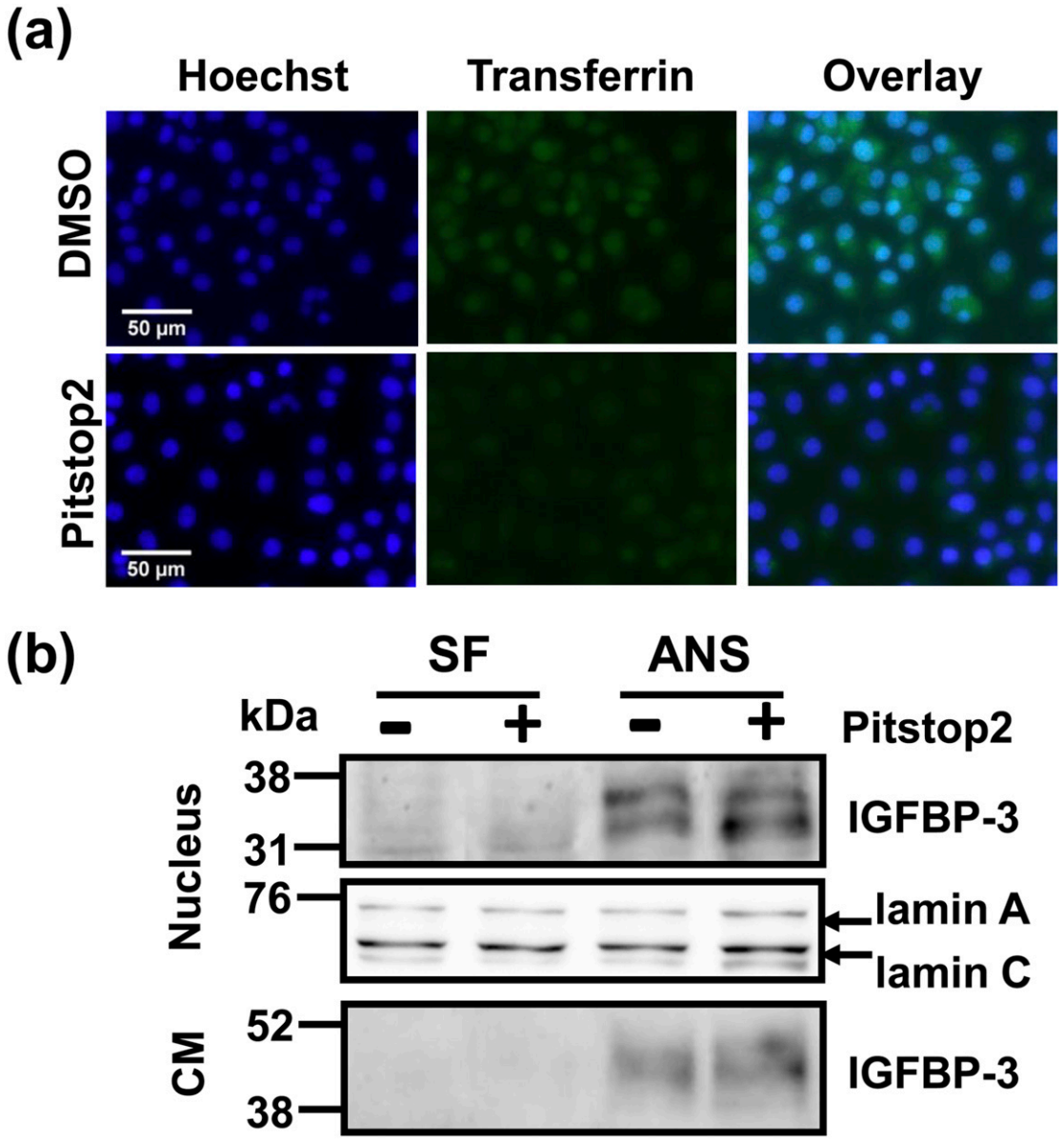

Figure 6. Secreted IGFBP-3 was not reinternalized. (a) To confirm that Pitstop 2 blocks clathrin-mediated endocytosis, cells were treated for 45 min + transferrin-FITC (25 μg/mL) ± Pitstop 2. Cells were fixed in formalin, and then nuclei were stained with Hoechst. Images were acquired with an Olympus FSX100 microscope at 40× magnification. (b) Cells treated with ANS ± Pitstop 2 were fractionated and western immunoblotted for IGFBP-3 or lamin A/C. CM were collected and immunoblotted for IGFBP-3 to confirm that synthesis of IGFBP-3 was not affected. Results are representative of (a) two or (b) three experiments. DMSO, dimethyl sulfoxide.

To address the previous observation that the molecular weight of IGFBP-3 in CM was higher than that of IGFBP-3 present in the nuclear fraction, samples of CM, WCLs, and cytosolic and nuclear fractions were directly compared on SDS-PAGE gels [Fig. 8(b)]. Endogenous IGFBP-3 present in media conditioned by cells treated with ANS or DON migrated as a doublet at approximately 38 to 45 kDa, whereas intracellular IGFBP-3 ran as a doublet at 34 to 38 kDa. To determine whether these differences in size were due to differences in glycosylation status, CM samples were subjected to enzymatic digestion with Endo H or PNGase F. PNGase F deglycosylates all glycosylation types including complex sugars, whereas Endo H can reduce only noncomplex mannose or hybrid glycans. Digestion of CM with PNGase F decreased the molecular weight of IGFBP-3 to a diffuse band around 32 kDa

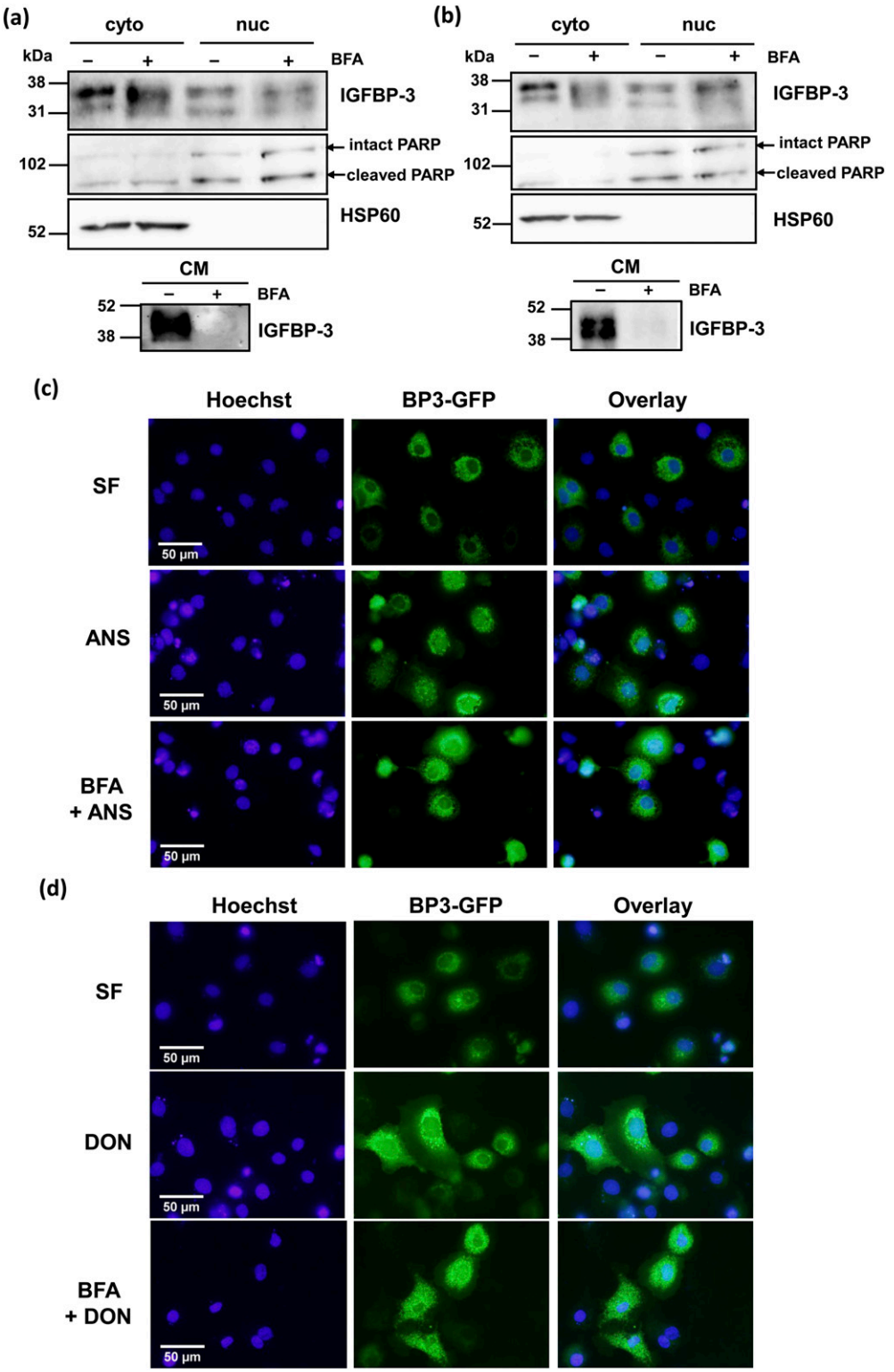

Figure 7. IGFBP-3 was not secreted before nuclear localization. MAC-T cells were treated with either (a) 0.1 μM ANS or (b) 1 μg/mL DON ± 10 μg/mL BFA. Cells were treated for 6 h with ANS or DON. BFA was added for the last 4 h of toxin treatment. Conditioned media were collected, and cells were fractionated. Samples were immunoblotted for IGFBP-3. PARP and HSP60 served as cytoplasmic (cyto) and nuclear (nuc) loading controls, respectively. Results are representative of three independent experiments. MAC-T cells transfected with IGFBP-3-GFP were treated with either (c) 0.1 μM ANS ± 10 μg/mL BFA for 1.5 h or

(d) 1 μg/mL DON ± 10 μg/mL BFA for 2 h. Cells were fixed in formalin, and then nuclei were stained with Hoechst. Images were acquired with an Olympus FSX100 microscope at 40× magnification. Images represent two independent experiments. BFA, brefeldin A.

and a more discrete band of 29 kDa [Fig. 8(c)], whereas digestion with Endo H had no effect on IGFBP-3 migration. In contrast, as shown in Fig. 8(d), intracellular IGFBP-3 was reduced by both Endo H and PNGase F to 29 and 32 kDa, respectively. Lighter bands of 29 kDa were also observed with PNGase F treatment. The patterns of deglycosylation of ANS-induced and DON-induced IGFBP-3 were similar. The ability of Endo H to deglycosylate intracellular IGFBP-3 (nuclear and cytoplasmic) but not IGFBP-3 from CM indicates that intracellular IGFBP-3 contains noncomplex mannose or hybrid glycans, whereas secreted IGFBP-3 carries complex glycosylation. Because the latter requires transit from the ER to the Golgi, intracellular IGFBP-3 is likely exiting the ER and localizing to the nucleus.

3. Discussion

ANS and DON are ribotoxins that have been used as a model in our laboratory to investigate the intrinsic apoptotic pathway in the MEC line MAC-T. We previously reported that ANS induced IGFBP-3 expression in MAC-T cells and that knockdown of IGFBP-3 attenuated the ability of ANS to induce intrinsic apoptosis [6]. We now report similar observations with the tricothecene DON, indicating that IGFBP-3 may be a general component of ribotoxic stress-induced apoptosis.

IGFBP-3 has had divergent effects on multiple cellular processes, including cellular proliferation, cell survival, and apoptosis, depending on cellular context [30, 34]. Many studies have implicated a role for nuclear IGFBP-3 in apoptosis, suggesting that cellular localization may be important in determining its cellular function. In the present work, we show that endogenous IGFBP-3 localized to the nucleus in ribotoxin-treated cells, as shown by others with TGF-β [7, 9]. Examination of the cellular distribution of transfected IGFBP-3 in cells treated with ribotoxin ruled out passive diffusion through nuclear pores, supporting an active mechanism of transport.

Work with exogenous purified protein or transfected IGFBP-3 has shown that the bipartite NLS is required for its nuclear transport [11, 16, 32, 35]. Schedlich *et al.* [32] showed that NLS associates with importin-β to mediate nuclear transport of exogenous IGFBP-3 in permeabilized Chinese hamster ovary cells, whereas knockdown of importin-β with siRNA reduced nuclear import of exogenous IGFBP-3 in osteosarcoma cells [14]. The present work extends these observations by showing that an external signal can specifically induce an association between endogenous IGFBP-3 and importin-β and that blocking this association with importazole prevents its nuclear localization. The mechanism by which ANS and DON induce this association is unknown, but the data clearly show that a specific signal is required because IGFBP-3 does not localize to the nucleus in its absence.

Although several studies have examined how exogenous IGFBP-3 can enter cells [9, 14, 36], work from the Cohen laboratory indicated that endogenous IGFBP-3 secreted in response to TGF-β in PC3 cells can be reinternalized and directed to the nucleus via endocytic mechanisms [9, 37]. Researchers showed that blocking transferrin receptor–mediated endocytosis and inhibiting caveolae formation prevented IGFBP-3 reuptake into the cell. In contrast to these reports indicating that IGFBP-3 is first secreted and then reinternalized, several lines of evidence presented here indicate that IGFBP-3 produced in response to ANS or DON escaped the secretory pathway between the ER and Golgi and was transported to the nucleus instead of being secreted. First, blocking CME with the inhibitor Pitstop 2 failed to decrease nuclear localization of IGFBP-3 in response to ANS. Pitstop 2 inhibits internalization of the transferrin receptor [33], which is a CME cargo protein, and has also been reported to inhibit clathrin-independent endocytosis [38]. Second, IGFBP-3 nuclear localization was unaffected by treatment with brefeldin A. If IGFBP-3 was first secreted and then reinternalized, less IGFBP-3 should be present in the nucleus of cells exposed to brefeldin A. Third, nuclear IGFBP-3 was

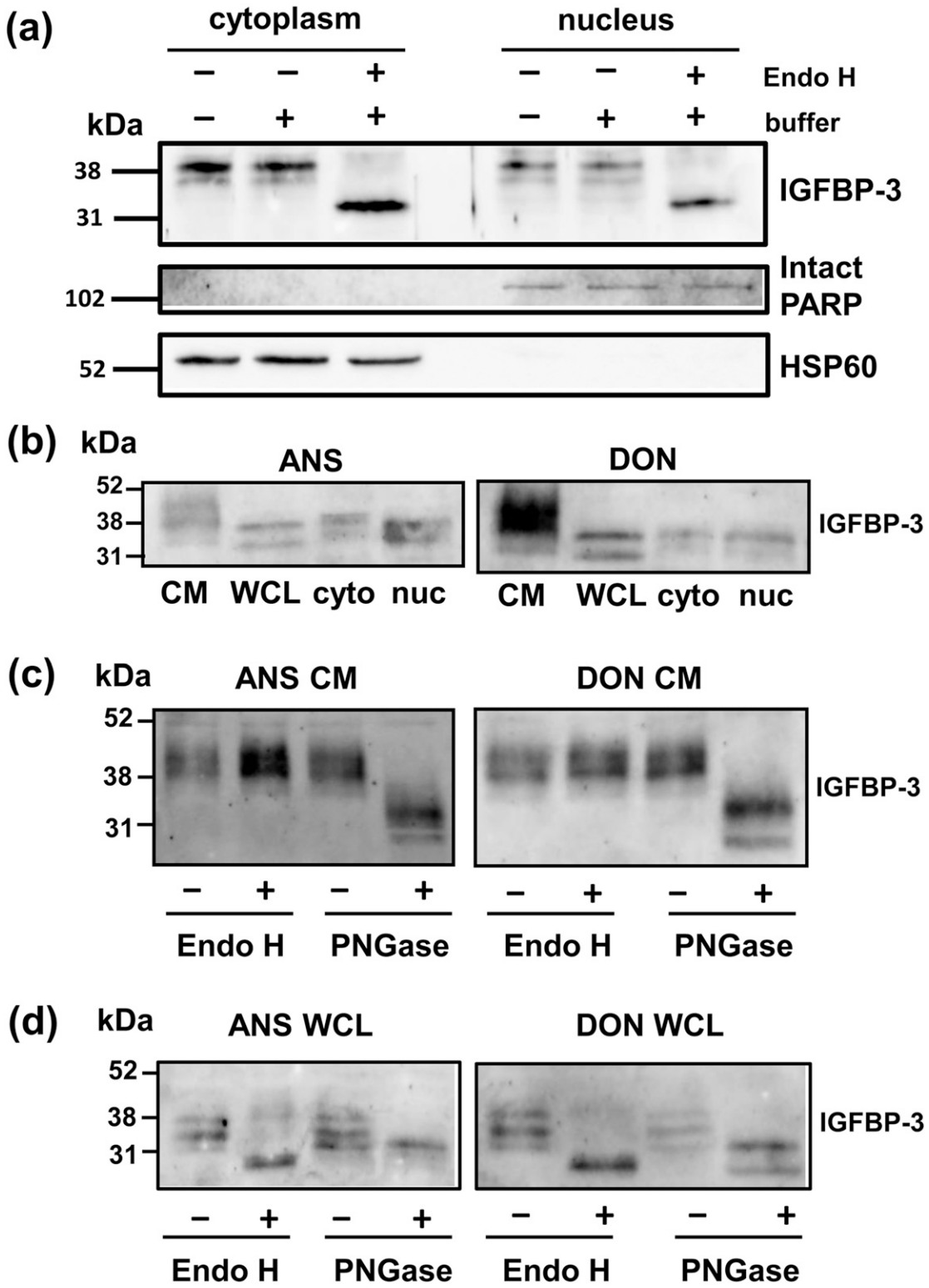

Figure 8. IGFBP-3 was differentially glycosylated depending on cellular localization. (a) Cells transfected with IGFBP-3-His were treated for 6 h with ANS to induce nuclear localization of IGFBP-3 and then fractionated. Lysates were treated ± Endo H to deglycosylate proteins, separated by SDS-PAGE, and immunoblotted for IGFBP-3. PARP and HSP60 served as controls for nuclear and cytoplasmic loading, respectively. Results are representative of two independent experiments. (b) Cells were treated with 0.1 μM ANS or 1 μg/mL DON. After 6 h, cells were fractionated or

lysed to collect WCLs. After 18 h, CM were collected. Membranes were immunoblotted for IGFBP-3. (c) Cells were treated for 18 h + 0.1 μM ANS or 1 μg/mL DON and CM were collected, or (d) cells were treated for 6 h + 0.1 μM ANS or 1 μg/mL DON and WCLs were collected. Samples were treated ± Endo H or PNGase F to deglycosylate proteins, separated by SDS-PAGE, and immunoblotted for IGFBP-3. cyto, cytoplasmic; nuc, nuclear.

glycosylated, indicating that it passed through at least part of the secretory pathway. Although both secreted IGFBP-3 and intracellular IGFBP-3 were glycosylated, IGFBP-3 collected from CM after ribotoxin treatment consistently migrated at a higher molecular weight than intracellular IGFBP-3 did. The deglycosylation enzymes Endo H and PNGase F have been used to distinguish between *N*-linked glycosylation types [39]. ER proteins that carry a high-mannose glycan or a hybrid glycan can be reduced by Endo H to a nonglycosylated form. In contrast, proteins edited in the cisternae of the Golgi are unable to be cleaved with Endo H because of their complex-type glycans. We determined that secreted IGFBP-3 in the CM was Endo H resistant and thus contained complex-type glycans, whereas intracellular IGFBP-3 was Endo H sensitive and thus contained only noncomplex high mannose or hybrid glycans. Collectively, these findings indicate that nuclear IGFBP-3 did not travel through the Golgi.

As mentioned previously, *N*-glycan processing occurs in the ER, where cellular machinery orchestrates quality control mechanisms and delegates proteins toward their proper fate [40]. Misfolded or unassembled multisubunit proteins are recognized by chaperones and associated factors with the help of *N*-linked glycosylation. Targeted proteins are then shuttled through the endoplasmic reticulum-associated degradation (ERAD) machinery for proteasomal degradation in the cytoplasm. This requires retrotranslocation through a Sec61 channel and deglycosylation by PNGase [41, 42]. Some proteins, such as ricin, are known to use the ERAD machinery to escape the ER [43]. The active subunit of ricin (RTA) then escapes proteasomal degradation because of a lack of lysine residues required for ubiquitination [44, 45]. However, because IGFBP-3 contains a number of C-terminal lysine residues, it is unclear how it would escape proteasomal degradation if it used ERAD to escape the ER. Another example of a protein that can escape its normal cellular location is calreticulin. Calreticulin, a calcium-binding ER resident chaperone, has been found in the cytosol and the nucleus and on the cell surface, indicating that it somehow escapes ER retention [46]. A retrotranslocation model for calreticulin has been proposed in which ER calcium depletion triggers a change in conformation that allows calreticulin to be recognized by the ERAD machinery [47].

Although IGFBP-3 is a secreted protein, its presence in the nucleus indicates it also may have intracrine effects on the cell. Because nonsecreted IGFBP-3 can localize to the nucleus in MAC-T cells and other cell lines [15, 16], it is likely that intracrine effects play a role in IGFBP-3–mediated apoptosis. Glycosylation status and complexity of glycosylation affect intracellular trafficking and the activity of several proteins; thus, glycosylation may play a role in deciding the fate of IGFBP-3 as a tag to direct compartmentalization, specifically toward ERAD machinery in the ER [48–51]. Interestingly, a role for IGFBP-3 in autophagy has been described in breast cancer cells [52]. The authors found this effect to be mediated by binding of IGFBP-3 to GRP78 in the ER, with binding increased by the underglycosylation of IGFBP-3 resulting during stress. In addition, glycosylation is known to affect protein folding [40] and may serve to reveal or conceal an NLS for IGFBP-3. Future work will focus on determining the mechanisms by which IGFBP-3 escapes the secretory pathway in ribotoxin-treated cells. Studies examining the effect of exogenous IGFBP-3 on apoptosis have used recombinant nonglycosylated IGFBP-3. Therefore, it will also be important to determine whether the underglycosylated form plays a unique role in apoptosis relative to the fully glycosylated form and if this is a universal mechanism across cell types or if it is limited to mammary epithelial cells.

Acknowledgments

Financial Support: This work was supported by National Research Initiative Competitive grant no. 2009-35206-05210 from the USDA National Institute of Food and Agriculture (to W.S.C.) and New Jersey Agricultural Experiment Station grant no. NJ06148 (to W.S.C.).

Correspondence: Wendie S. Cohick, PhD, Department of Animal Sciences, Rutgers, The State University of New Jersey, 59 Dudley Road, New Brunswick, New Jersey 08901-8520. E-mail: cohick@sebs.rutgers.edu.

Disclosure Summary: The authors have nothing to disclose.

References and Notes

1. Boutinaud M, Guinard-Flamenta J, Jammes H. The number and activity of mammary epithelial cells, determining factors for milk production. *Reprod Nutr Dev*. 2004;**44**(5):499–508.
2. Annen EL, Fitzgerald AC, Gentry PC, McGuire MA, Capuco AV, Baumgard LH, Collier RJ. Effect of continuous milking and bovine somatotropin supplementation on mammary epithelial cell turnover. *J Dairy Sci*. 2007;**90**(1):165–183.
3. Capuco AV, Ellis SE, Hale SA, Long E, Erdman RA, Zhao X, Paape MJ. Lactation persistency: insights from mammary cell proliferation studies. *J Anim Sci*. 2003;**81**(15 Suppl 3):18–31.
4. Capuco AV, Wood DL, Baldwin R, Mcleod K, Paape MJ. Mammary cell number, proliferation, and apoptosis during a bovine lactation: relation to milk production and effect of bST. *J Dairy Sci*. 2001; **84**(10):2177–2187.
5. Cohick WS, Clemmons DR. The insulin-like growth factors. *Annu Rev Physiol*. 1993;**55**(1):131–153.
6. Leibowitz BJ, Agostini-Dreyer A, Jetzt AE, Krumm CS, Cohick WS. IGF binding protein-3 mediates stress-induced apoptosis in non-transformed mammary epithelial cells. *J Cell Physiol*. 2013;**228**(4): 734–742.
7. Xi G, Hathaway MR, White ME, Dayton WR. Localization of insulin-like growth factor (IGFBP)-3 in cultured porcine embryonic myogenic cells before and after TGF-β1 treatment. *Domest Anim Endocrinol*. 2007;**33**(4):422–429.
8. Granata R, Trovato L, Garbarino G, Taliano M, Ponti R, Sala G, Ghidoni R, Ghigo E. Dual effects of IGFBP-3 on endothelial cell apoptosis and survival: involvement of the sphingolipid signaling pathways. *FASEB J*. 2004;**18**(12):1456–1458.
9. Lee KW, Liu B, Ma L, Li H, Bang P, Koeffler HP, Cohen P. Cellular internalization of insulin-like growth factor binding protein-3: distinct endocytic pathways facilitate re-uptake and nuclear localization. *J Biol Chem*. 2004;**279**(1):469–476.
10. Agostini-Dreyer A, Jetzt AE, Stires H, Cohick WS. Endogenous IGFBP-3 mediates intrinsic apoptosis through modulation of Nur77 phosphorylation and nuclear export. *Endocrinology*. 2015;**156**(11): 4141–4151.
11. Schedlich LJ, Young TF, Firth SM, Baxter RC. Insulin-like growth factor-binding protein (IGFBP)-3 and IGFBP-5 share a common nuclear transport pathway in T47D human breast carcinoma cells. *J Biol Chem*. 1998;**273**(29):18347–18352.
12. Xu C, Bailly-Maitre B, Reed JC. Endoplasmic reticulum stress: cell life and death decisions. *J Clin Invest*. 2005;**115**(10):2656–2664.
13. Zhou HR, He K, Landgraf J, Pan X, Pestka JJ. Direct activation of ribosome-associated double-stranded RNA-dependent protein kinase (PKR) by deoxynivalenol, anisomycin and ricin: a new model for ribotoxic stress response induction. *Toxins (Basel)*. 2014;**6**(12):3406–3425.
14. Micutkova L, Hermann M, Offterdinger M, Hess MW, Matscheski A, Pircher H, Mück C, Ebner HL, Laich A, Ferrando-May E, Zwerschke W, Huber LA, Jansen-Dürr P. Analysis of the cellular uptake and nuclear delivery of insulin-like growth factor binding protein-3 in human osteosarcoma cells. *Int J Cancer*. 2012;**130**(7):1544–1557.
15. Bhattacharyya N, Pechhold K, Shahjee H, Zappala G, Elbi C, Raaka B, Wiench M, Hong J, Rechler MM. Nonsecreted insulin-like growth factor binding protein-3 (IGFBP-3) can induce apoptosis in human prostate cancer cells by IGF-independent mechanisms without being concentrated in the nucleus. *J Biol Chem*. 2006;**281**(34):24588–24601.
16. Santer FR, Bacher N, Moser B, Morandell D, Ressler S, Firth SM, Spoden GA, Sergi C, Baxter RC, Jansen-Dürr P, Zwerschke W. Nuclear insulin-like growth factor binding protein-3 induces apoptosis and is targeted to ubiquitin/proteasome-dependent proteolysis. *Cancer Res*. 2006;**66**(6):3024–3033.
17. RRID:AB_2341188.
18. RRID:AB_2068144.
19. RRID:AB_2160739.
20. RRID:AB_733032.
21. RRID:AB_2133989.
22. RRID:AB_648154.
23. RRID:AB_914704.

24. RRID:AB_2336177.
25. RRID:AB_772206.
26. Huynh HT, Robitaille G, Turner JD. Establishment of bovine mammary epithelial cells (MAC-T): an in vitro model for bovine lactation. *Exp Cell Res*. 1991;**197**(2):191–199.
27. RRID:AB_2752245.
28. Cohick WS, Turner JD. Regulation of insulin-like growth factor binding protein synthesis by a bovine mammary epithelial cell line. *J Endocrinol*. 1998;**157**:327–336.
29. Grill CJ, Sivaprasad U, Cohick WS. Constitutive expression of IGF-binding protein-3 by mammary epithelial cells alters signaling through Akt and p70S6 kinase. *J Mol Endocrinol*. 2002;**29**(1):153–162.
30. Leibowitz BJ, Cohick WS. Endogenous IGFBP-3 is required for both growth factor-stimulated cell proliferation and cytokine-induced apoptosis in mammary epithelial cells. *J Cell Physiol*. 2009;**220**(1): 182–188.
31. Schmeits PC, Katika MR, Peijnenburg AA, van Loveren H, Hendriksen PJ. DON shares a similar mode of action as the ribotoxic stress inducer anisomycin while TBTO shares ER stress patterns with the ER stress inducer thapsigargin based on comparative gene expression profiling in Jurkat T cells. *Toxicol Lett*. 2014;**224**(3):395–406.
32. Schedlich LJ, Le Page SL, Firth SM, Briggs LJ, Jans DA, Baxter RC. Nuclear import of insulin-like growth factor-binding protein-3 and -5 is mediated by the importin β subunit. *J Biol Chem*. 2000; **275**(31):23462–23470.
33. von Kleist L, Stahlschmidt W, Bulut H, Gromova K, Puchkov D, Robertson MJ, MacGregor KA, Tomilin N, Pechstein A, Chau N, Chircop M, Sakoff J, von Kries JP, Saenger W, Kräusslich HG, Shupliakov O, Robinson PJ, McCluskey A, Haucke V. Role of the clathrin terminal domain in regulating coated pit dynamics revealed by small molecule inhibition. *Cell*. 2011;**146**(3):471–484.
34. Johnson MA, Firth SM. IGFBP-3: a cell fate pivot in cancer and disease. *Growth Horm IGF Res*. 2014; **24**(5):164–173.
35. Oufattole M, Lin SW, Liu B, Mascarenhas D, Cohen P, Rodgers BD. Ribonucleic acid polymerase II binding subunit 3 (Rpb3), a potential nuclear target of insulin-like growth factor binding protein-3. *Endocrinology*. 2006;**147**(5):2138–2146.
36. Ainscough SL, Feigl B, Malda J, Harkin DG. Discovery and characterization of IGFBP-mediated endocytosis in the human retinal pigment epithelial cell line ARPE-19. *Exp Eye Res*. 2009;**89**(5): 629–637.
37. Weinzimer SA, Gibson TB, Collett-Solberg PF, Khare A, Liu B, Cohen P. Transferrin is an insulin-like growth factor-binding protein-3 binding protein. *J Clin Endocrinol Metab*. 2001;**86**(4):1806–1813.
38. Dutta D, Williamson CD, Cole NB, Donaldson JG. Pitstop 2 is a potent inhibitor of clathrin-independent endocytosis. *PLoS One*. 2012;**7**(9):e45799.
39. Shen W, Xiao Z, Shen J, Gao C. Analysis of golgi-mediated protein traffic in plant cells. *Methods Mol Biol*. 2017;**1662**:75–86.
40. Benyair R, Ogen-Shtern N, Lederkremer GZ. Glycan regulation of ER-associated degradation through compartmentalization. *Semin Cell Dev Biol*. 2015;**41**:99–109.
41. Spiro RG. Role of N-linked polymannose oligosaccharides in targeting glycoproteins for endoplasmic reticulum-associated degradation. *Cell Mol Life Sci*. 2004;**61**(9):1025–1041.
42. Vembar SS, Brodsky JL. One step at a time: endoplasmic reticulum-associated degradation. *Nat Rev Mol Cell Biol*. 2008;**9**(12):944–957.
43. Bellisola G, Fracasso G, Ippoliti R, Menestrina G, Rosén A, Soldà S, Udali S, Tomazzolli R, Tridente G, Colombatti M. Reductive activation of ricin and ricin A-chain immunotoxins by protein disulfide isomerase and thioredoxin reductase. *Biochem Pharmacol*. 2004;**67**(9):1721–1731.
44. Deeks ED, Cook JP, Day PJ, Smith DC, Roberts LM, Lord JM. The low lysine content of ricin A chain reduces the risk of proteolytic degradation after translocation from the endoplasmic reticulum to the cytosol. *Biochemistry*. 2002;**41**(10):3405–3413.
45. Lord JM, Roberts LM, Lencer WI. Entry of protein toxins into mammalian cells by crossing the endoplasmic reticulum membrane: co-opting basic mechanisms of endoplasmic reticulum-associated degradation. *Curr Top Microbiol Immunol*. 2005;**300**:149–168.
46. Afshar N, Black BE, Paschal BM. Retrotranslocation of the chaperone calreticulin from the endoplasmic reticulum lumen to the cytosol. *Mol Cell Biol*. 2005;**25**(20):8844–8853.
47. Labriola CA, Conte IL, López Medus M, Parodi AJ, Caramelo JJ. Endoplasmic reticulum calcium regulates the retrotranslocation of *Trypanosoma cruzi* calreticulin to the cytosol. *PLoS One*. 2010;**5**(10): e13141.
48. Fishburn CS, Elazar Z, Fuchs S. Differential glycosylation and intracellular trafficking for the long and short isoforms of the D_2 dopamine receptor. *J Biol Chem*. 1995;**270**(50):29819–29824.

49. Penuela S, Bhalla R, Nag K, Laird DW. Glycosylation regulates pannexin intermixing and cellular localization. *Mol Biol Cell*. 2009;**20**(20):4313–4323.
50. Zaarour N, Demaretz S, Defontaine N, Mordasini D, Laghmani K. A highly conserved motif at the COOH terminus dictates endoplasmic reticulum exit and cell surface expression of NKCC2. *J Biol Chem*. 2009;**284**(32):21752–21764.
51. Weng TY, Chiu WT, Liu HS, Cheng HC, Shen MR, Mount DB, Chou CY. Glycosylation regulates the function and membrane localization of KCC4. *Biochim Biophys Acta*. 2013;**1833**(5):1133–1146.
52. Grkovic S, O'Reilly VC, Han S, Hong M, Baxter RC, Firth SM. IGFBP-3 binds GRP78, stimulates autophagy and promotes the survival of breast cancer cells exposed to adverse microenvironments. *Oncogene*. 2013;**32**(19):2412–2420.